JOURNAL OF SOLID STATE CHEMISTRY **127,** 109–118 (1996)
ARTICLE NO. 0363

Magnetic Properties of $Li_{1-x}Ni_{1+x}O_2(0 \lesssim x \lesssim 0.08)$

Kazunari Yamaura[1] and Mikio Takano

Institute for Chemical Research, Kyoto University, Uji, Kyoto-fu 611, Japan

and

Atsushi Hirano and Ryoji Kanno

Department of Chemistry, Faculty of Science, Kobe University, Kobe, Hyogo 657, Japan

Received March 15, 1996; in revised form July 19, 1996; accepted September 16, 1996

Magnetic properties of $Li_{1-x}Ni_{1+x}O_2$ ($0 \lesssim x \lesssim 0.08$) crystallizing in the α-$NaFeO_2$ structure were studied by SQUID magnetometry. A sample with $x \lesssim 0.01$ prepared from Li_2O_2 and $Ni_{0.77}O$ at 650°C follows the Curie–Weiss law from 350 to 80 K with μ_{eff} (effective Bohr magneton) of 1.91 μ_B and Θ (Weiss temperature) of +29.5 K. A spin glass-like thermomagnetic hysteresis with a cusp at 8 K was observed. Samples with larger x values exhibit ferromagnetic moments, typically 0.3 μ_B/Ni ($x \sim 0.08$) at 5 K. From these and other results we conclude that the dominant intra-Ni layer interaction is ferromagnetic and that excess Ni ions located in the Li layers introduce strong ferromagnetic inter-Ni layer interactions. Possible importance of orbital–spin coupling and frustration in orbital ordering will be raised to the magnetism of ideal $LiNiO_2$, in which Ni^{3+} ($S = 1/2$) ions with twofold orbital degeneracy form a ferromagnetic triangular lattice.

1. INTRODUCTION

Solid state chemistry of $LiNiO_2$ crystallizing in the α-$NaFeO_2$-type layered structure has been studied intensively since this compound is suitable for the insertion electrode of a low cost and high energy density rechargeable Li battery (1–3). On the other hand, magnetic properties of this compound and the solid solution $Li_{1-x}Ni_{1+x}O_2$ ($0 < x < 1$) have also been long studied (4–9). Goodenough *et al.* were motivated by a possibility of metallic ferromagnetism by the double exchange mechanism in the solid solution containing Ni^{2+} and Ni^{3+} (4), while Hirakawa *et al.* expected that a frustrated antiferromagnetic $S = 1/2$ triangular lattice might be realized in $LiNiO_2$ (5). The ideal rhombodhedral structure of $LiNiO_2$ ($R\bar{3}m$; Li, 3*a*; Ni, 3*b*; and O, 6*c*) is illustrated in Fig. 1, in which NiO_6 octahedra of trigonal symmetry share their edges to form a triangular Ni lattice such as depicted at the bottom of Fig. 1. Nonmagnetic Li layers (LL) alternate with the magnetic Ni layers (NL) along the ⟨111⟩ direction, making the inter-NL distance (4.73 Å) much longer than the intralayer Ni–Ni distance of 2.88 Å. Magnetic correlations between the Ni ions mediated by oxide ions have thus been considered two dimensional (2D) in nature.

Goodenough *et al.* assumed Ni^{3+} in the low spin state (t^6e^1) with an isotropic spin $S = 1/2$, while Hirakawa *et al.* assumed the high spin state (t^5e^2) leading to a low-lying Kramers doublet with a fictitious Ising spin $S = 1/2$. More recently, from X-ray absorption spectroscopic studies of NiO partially substituted with Li and Na, $M_yNi_{1-y}O$ (M = Li, Na), Kuiper *et al.* (10) and van Veenendaal and Sawatzky (11) claimed that holes doped into NiO by the aliovalent substitution resided on the oxygen sublattice. They and Mizokawa *et al.* (12) also suggested that the end members, $LiNiO_2$ and $NaNiO_2$, would be in the negative charge-transfer energy regime: $Ni^{2+}(O_6)^{-11}$, or $Ni^{2+}\underline{L}$ ($\underline{L}$, ligand hole), ($S = 1/2$) is a more realistic picture of the electronic ground state than $Ni^{3+}(O_6)^{-12}$ ($S = 1/2$). If this is the case, the M^+ and Ni^{2+} ions are ordered in the octahedral sites of the *fcc* lattice made of O^{2-} and O^- mixed at 1 : 1. They argued that the insulating nature of $LiNiO_2$ and $NaNiO_2$ might be explained in different ways including small band effects caused by the orthogonality of the Ni–O–Ni bonds and correlation effects between holes on the same oxygen site.

It is known to be difficult to obtain stoichiometric $LiNiO_2$ free from the presence of excess Ni ions at 3*a* sites (1–3). It should be emphasized here that such a Ni ion creates three Ni(3*b*, upper layer)–O–Ni(3*a*)–O–Ni(3*b*, lower layer) bonds, which are almost linear and, therefore, would be much stronger magnetically than the intralayer Ni(3*b*)–O–Ni(3*b*) bond bent at nearly 90° (see Fig. 1) (13). A wide range of different behavior reported by several groups

[1] To whom correspondence should be addressed.

0022-4596/96 $18.00

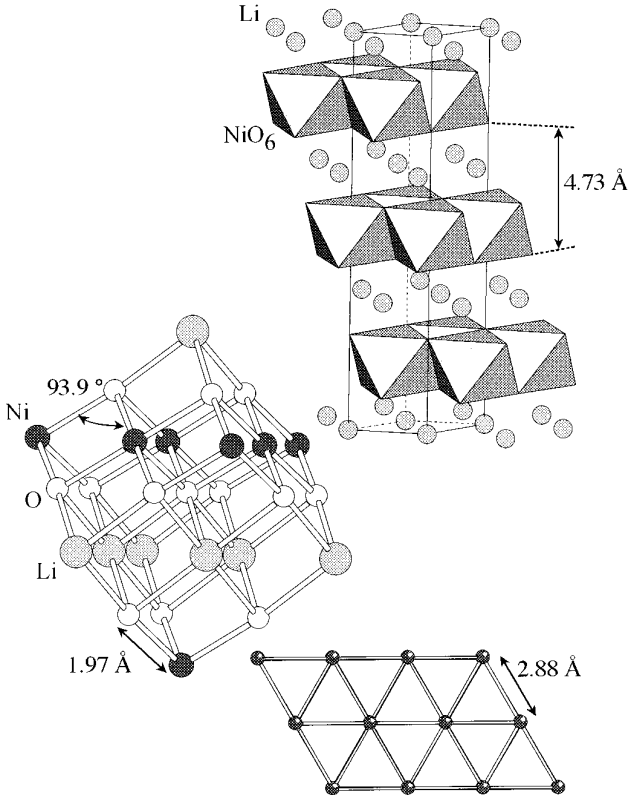

FIG. 1. α-$NaFeO_2$ type structure ($R\bar{3}m$). A hexagonal unit cell is shown with the solid and dotted lines (top). The lattice constants for $x \lesssim 0.01$ are $a = 2.876$ Å and $c = 14.191$ Å [2]. The Ni–O and Li–O bonds constituting the face centered rhombohedral lattice are also shown (middle). The NiO_6 octahedra of trigonal symmetry share their edges to form a triangular Ni lattice such as depicted at the bottom.

might indicate the importance of such extrinsic effects resulting from difficulties in sample preparation. The electrochemical performance is also known to be seriously affected by this kind of defect (3). To clarify the intrinsic magnetism and intrinsic electrochemical properties, it is essentially important to suppress the disordering. For that purpose we studied the phase relation between $LiNiO_2$ and related compounds (2, 9), examining different synthesizing conditions including heating process, atmosphere, and starting materials. As a result we recently obtained a sample which showed the simplest magnetic behavior we ever observed. The magnetic properties of this and other samples will be presented in this paper.

2. SAMPLE PREPARATION AND CHARACTERIZATION

We used 95.3% pure Li_2O_2 and two kinds of nickel oxides as starting materials. The low purity of Li_2O_2 comes from the presence of Li_2O. One of the nickel oxides is a 99.9% pure commercially available green powder of $Ni_{1.0}O$, while the other is $Ni_{0.77}O$, a black powder prepared by heating $Ni(OH)_2$ at 300°C in a flowing argon stream for 30 min (use of oxygen instead of argon gives essentially the same powder). The hydroxide was obtained as a deposit from an aqueous solution of $NiCl_2 \cdot 6H_2O$ (0.5 *N*) to which an aqueous solution of NaOH (1 *N*) was added. The precipitate was filtered out, washed with distilled water, dried, and thermally decomposed. Thermogravimetric analysis showed that $Ni_{0.77}O$ was obtainable at relatively low temperatures, while it was reduced to $Ni_{1.0}O$ at ~600°C in the same flowing argon atmosphere (at ~700°C when oxygen is used). This $Ni_{0.77}O$ is not hexagonal $Ni_{2/3}O$ (14) but is a cubic rock salt-type oxide (15). According to our X-ray powder diffraction (XRD) study, the unit cell volume of $Ni_{0.77}O$ is larger by 1.2% than that of $Ni_{1.0}O$. Furthermore, remarkable peak broadening that suggested the particles were very fine was observed in the XRD pattern. In consistency with this, use of scanning and transmission electron microscopes revealed a typical particle size of less than 1 μm for $Ni_{0.77}O$ and on the order of 10 μm for $Ni_{1.0}O$.

Li_2O_2 and one of the nickel oxides were weighed, mixed, and pelletized in a glove box filled with argon and then heated at a fixed temperature between 400 and 900°C for 48 hr in moisture-free flowing oxygen. Because of a relatively high fugacity of Li at elevated temperatures, Li_2O_2 was used in excess, by 5 at.% typically, in the starting mixtures. This $Ni_{0.77}O$ is proved to be quite reactive: $Ni_{1.0}O$ does not react with Li_2O_2 below 600°C, but $Ni_{0.77}O$ does even at 400°C.

Final compositions and structural parameters of these samples were determined using XRD and neutron powder diffraction (ND) at room temperature. The XRD patterns were obtained with Cu$K\alpha$ radiation using a specially designed sample holder filled with argon to prevent moisture attack. ND measurements were made for several selected samples, which were vacuum-sealed in vanadium cells, at Tokai Establishment of Japan Atomic Energy Research Institute using neutrons of 1.7691 Å monochromatized with a pyrolytic graphite crystal. Rietveld analysis using the RIETAN program (16) was done for refinements. The XRD and ND data indicated the α-$NaFeO_2$ structure in which a small amount of Ni substitutes for Li at 3*a* site: The magnetic NLs were perfect within experimental error, while the nonmagnetic LLs were contaminated slightly with Ni to form $Li_{1-x}Ni_x$. The x values determined by the Rietveld analysis for the samples prepared from $Ni_{1.0}O$ and Li_2O_2 are plotted against the synthesizing temperature in Fig. 2, where the XRD and ND results are shown with open circles and closed circles, respectively. The open squares represent the values calculated from the XRD intensity ratio of $(I(006) + I(012))/I(101)$ as proposed by Dahn *et al.* (1). These different estimations do not agree exactly with each other but reveal consistently that Ni content at 3*a* site increases from 0.01 or less (650 and

700°C) to ~0.08 (900°C) with increasing the heating temperature. We should note here that the present characterization did not detect any anion nonstoichiometry. Further details including the phase relation and the composition dependence of crystallographic parameters are given elsewhere (2, 9).

The sample prepared from Li_2O_2 and $Ni_{0.77}O$ at 650°C (sample I) showed also essentially the same XRD refinement results of $x \lesssim 0.01$ as those for that prepared from $Ni_{1.0}O$ at 650°C (sample II). However, the magnetic properties of sample I were found to be considerably different from those of sample II and also from the previously reported data as shown below.

3. MAGNETIC PROPERTIES

3.1. Previous Results

A variety of magnetic behavior has been reported for "$LiNiO_2$" of different qualities, while we refer here mainly to three typical recent results. Hirota *et al.* (7) used three kinds of X-ray pure samples prepared from Li_2O_2 and NiO at 850°C in a stream of pure dried oxygen, the compositions of which were estimated to be $x = 0.056$, 0.096, and 0.107 from their unit cell volumes. For every composition, there were three kinds of magnetic anomalies at $T_{N1} \sim T_{N3}$ ($T_{N1} \sim 240$ K $> T_{N3} > T_{N2}$). Above T_{N1} susceptibility followed the Curie–Weiss law with $S = 0.546$ ($\mu_{eff} =$ 1.84 μ_B) and $\Theta = 79.3$ K typically. For $T_{N3} \leq T \leq T_{N1}$, magnetization was not linear to external field and increased exponentially with decreasing temperature. T_{N3} rose from ~70 K to ~100 K (not specified) as x increased. The temperature range $T_{N2} \leq T \leq T_{N3}$ was characterized by an even faster increase in magnetization at lower temperatures. ac susceptibility showed a huge peak at T_{N2}. This temperature was raised from 34 to 67 K as x increased. For $T \leq T_{N2}$, magnetization tended to saturate at lower temperatures. At the same time, a relaxation phenomenon with a long time constant was observed below T_{N2}.

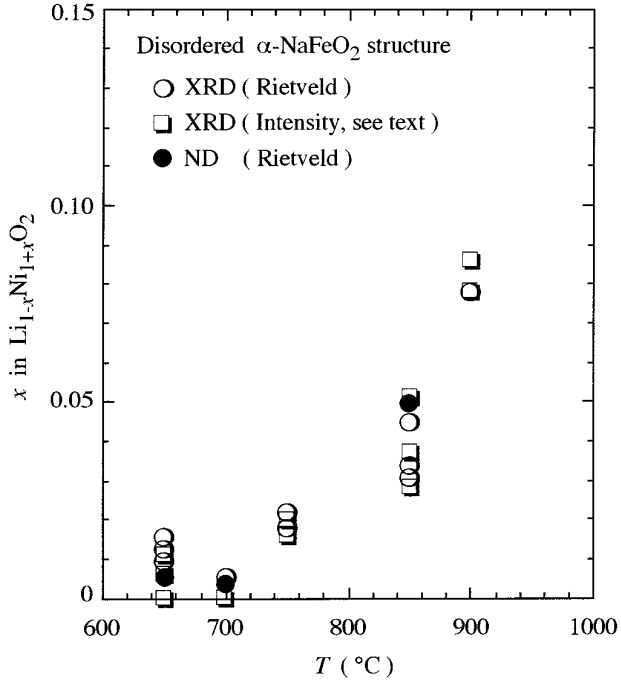

FIG. 2. Dependence of x against synthesis temperature for $Li_{1-x}Ni_{1+x}O_2$ prepared from Li_2O_2 and $Ni_{1.0}O$.

The samples studied by Reimers *et al.* (8) included two nearly stoichiometric samples prepared from $LiOH \cdot H_2O$ and NiO. The final heat treatment was carried out at 650°C for 4 hr in CO_2-free air with different humidities. Susceptibility showed Curie–Weiss behavior above 220 K with μ_{eff} and Θ of 2.1 μ_B and 26 K, respectively, for one sample and 2.2 μ_B and 2 K for the other sample. Deviation from the Curie–Weiss law was observed in a greater or lesser degree below 220 K for both these samples. The deviation below 220 K seems to correspond to the T_{N1} anomaly reported by Hirota *et al.* (7). The most remarkable result was that both these samples showed spin glass-like hysteretic behavior at low temperatures which had not been reported before them. A well-defined cusp appeared at 9 K in the temperature dependence of magnetization measured at 10 Oe after zero-field cooling, while magnetization monotonically increased when the samples were field cooled at 500 Oe. When the field was removed after cooling to 5 K, magnetization decayed slowly, in support of the spin glass picture.

Both these groups commonly assumed intra-NL antiferromagnetic frustration. Hirota *et al.* (7) assigned the anomalous behavior below T_{N1} to successive development of spin correlation from a planar short range order, a three dimensional short range order, and to a new type of frozen state which is different from ordinary spin glass. Reimers *et al.* (8) presumed a classical ground state with a triangular spin arrangement for the ideal NLs, while they argued that the ground state was replaced by the spin glass state as a result of the mixed effects of the intra-NL antiferromagnetic frustration, random introduction of a ferromagnetic Ni(3*a*)–O–Ni(3*b*) interaction (J'), and the inter-NL ferromagnetic interaction (J'', intrinsic interaction not mediated by Ni(3*a*) ions). The deviation from the Curie–Weiss law below 220 K was assigned to these ferromagnetic interactions J' and J''.

On the other hand, according to Kemp *et al.* (6), $LiNiO_2$ prepared from Li_2CO_3 (3% excess) and NiO at 800°C in pure dry oxygen behaved as a weakly coupled 2D Ising ferromagnet. The ferromagnetic intra-NL interaction was concluded from a positive Weiss temperature of 60 K and the appearance of a small spontaneous magnetization at 4.2 K. It is interesting to notice that although similar mag-

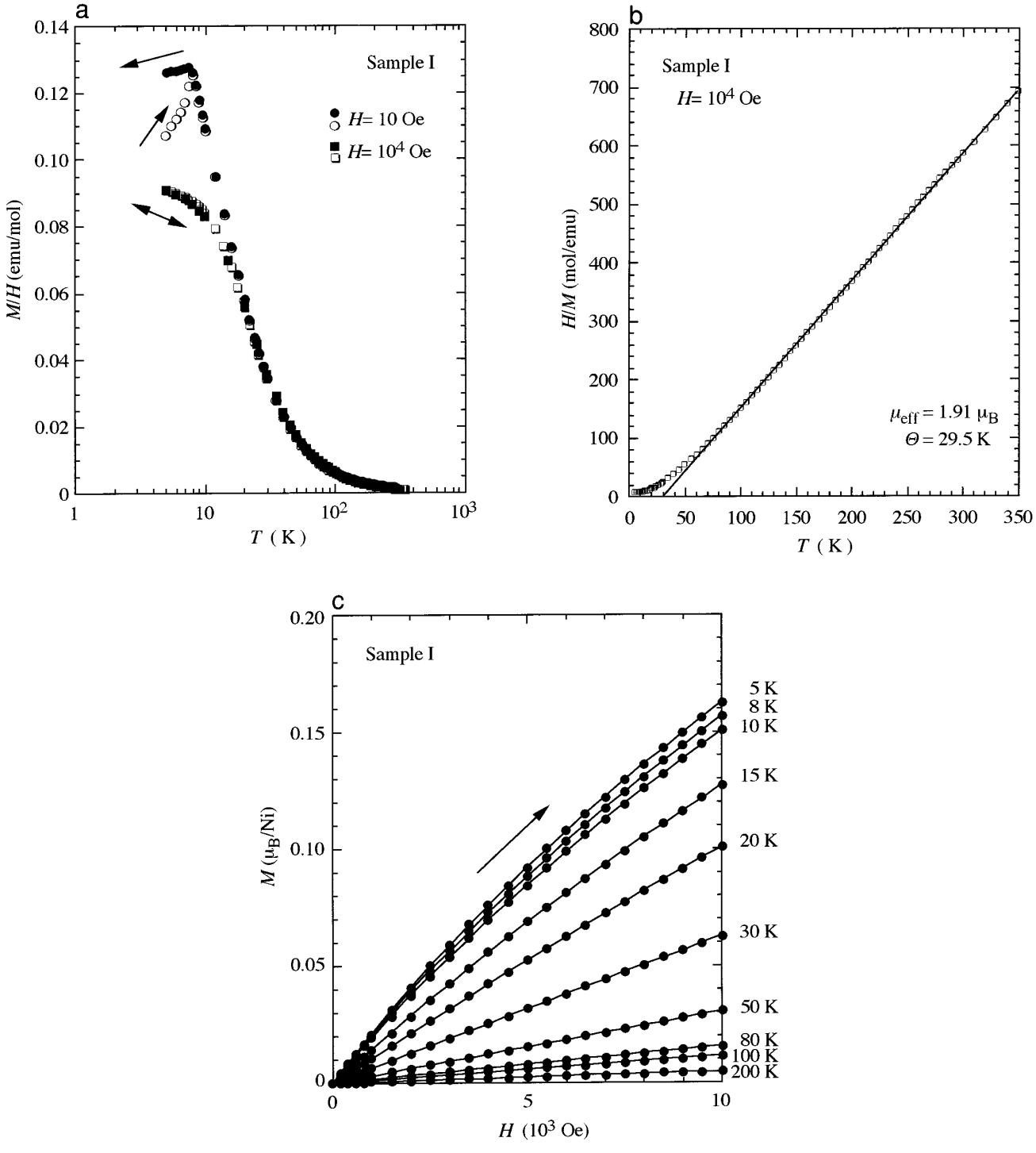

FIG. 3. (a) Temperature dependence of magnetization (M) for sample I ($x \lesssim 0.01$) prepared at 650°C from Li_2O_2 and $Ni_{0.77}O$. The circles and squares represent the results at $H = 10$ and 10^4 Oe, respectively, while the closed and open marks correspond to measurements on field cooling and on heating after zero-field cooling, respectively. (b) H/M at $H = 10^4$ for sample I. The linear line represents Curie–Weiss behavior with $\mu_{eff} = 1.91\ \mu_B$ and $\Theta = 29.5$ K. The temperature independent term was found to be negligibly small, 4.5×10^{-5} emu/mol. (c) Field dependence of magnetization for sample I at different fixed temperatures. The sample was zero-field cooled from room temperature to a desired temperature and then field was applied stepwise up to 10^4 Oe. The solid lines are guides for the eyes.

netic features were included in the very detailed measurements by Hirota *et al.*, these two groups reached different conclusions.

3.2. Present Work

Magnetic measurements in the present work were performed with a SQUID magnetometer (Quantum Design, MPMS2). Small magnetic fields of ~10 Oe were calibrated carefully by using pure Pb metal, a superconductor below 7.2 K. The data for sample I with $x \lesssim 0.01$ prepared from $Ni_{0.77}O$ and Li_2O_2 at 650°C are shown in Figs. 3a–3c. The circles and squares represent the results at $H = 10$ Oe and 1.00×10^4 Oe, respectively, while the closed and open marks correspond to measurements on field cooling and measurements on heating after zero-field cooling, respectively. The magnetization measured at 10^4 Oe gradually saturates at lower temperatures, without showing any sharp anomaly or hysteresis. On the other hand, the data at 10 Oe shows a cusp at 8 K and a well-defined hysteresis below that. The inverse, H/M, at $H = 10^4$ Oe is plotted in Fig. 3b, which can be fitted to the Curie–Weiss law between 350 and 80 K with parameter values $\mu_{\text{eff}} = 1.91\ \mu_B$ and $\Theta = 29.5$ K. The temperature-independent term is negligibly small, 4.5×10^{-5} emu/mol. The value of μ_{eff} is slightly larger than expected from $g = 2$ and $S = 1/2$ ($1.73\ \mu_B$). The dominant interaction, J, was estimated to be +8.1 K (ferromagnetic) from the second term of the high temperature expansion of inverse susceptibility based on a mean field approximation in which only the nearest neighbor interaction was considered (17–19). Much quantitative importance should not be attached to this simple estimation, but we find no evidence for the standard antiferromagnetic intra-NL interaction.

The field dependence of magnetization for the same sample at different fixed temperatures is shown in Fig. 3c. The sample was zero-field cooled from 300 K to a desired temperature and then field was applied stepwise up to 10^4 Oe. Below 20 K nonlinearity was clearly observed, suggesting the presence of a small ferromagnetic contribution. In consistency with this, the M/H vs T curves at $H = 10$ Oe and 10^4 Oe separate from each other below 20 K in Fig. 3a. Both Hirota *et al.* (7) and Reimers *et al.* (8) observed relaxation of magnetization over macroscopic time scales, but magnetization of sample I cooled at $H = 10^4$ Oe to 5 K relaxed to one hundredth or less within 1 min before the measurement of the relaxation started.

For comparison, corresponding data for sample II with $x \lesssim 0.01$ prepared at 650°C using $Ni_{1.0}O$ instead of $Ni_{0.77}O$ are shown in Figs. 4a–4c. The most important feature of this sample is that there is a well-defined hysteresis below 220 K in the M/H vs T curve measured at $H = 10$ Oe. Behavior around this temperature is enlarged in Fig. 4b. The measurement at $H = 10^4$ Oe does not show any hysteresis at 220 K, while a deviation from the Curie–Weiss law can be clearly seen below 240 K in Fig. 4c. This deviation seems to be essentially the same as the 240-K anomaly reported generally by Hirota *et al.* (7), Reimers *et al.* (8), and others. Another anomaly at 7.5 K is almost the same as that for sample I. For this sample also, we did not find any relaxation phenomenon at 5 K.

3.3. Magnetic Properties of $Li_{1-x}Ni_{1+x}O_2$ with $x \gtrsim 0.04$

To make clear the systematic dependence of the effects of the Ni-for-Li substitution at the 3*a* site, the magnetic behavior of two other samples with $x \sim 0.04$ and 0.08 will be described. Typical M/H vs T curves obtained for the sample with $x \sim 0.04$ prepared using $Ni_{1.0}O$ at 850°C are shown in Fig. 5a. Again the difference between the field cooled and zero-field cooled data is important for $H = 10$ Oe. One would notice first that for this sample there are no such anomalies as seen at 8 K for samples I and II and at 240 K for sample II, but there is an anomaly at 100 K. Below this temperature the data at $H = 10$ Oe deviates from those at $H = 10^4$ Oe. As compared in Fig. 5b, the temperature of this anomaly rises to 140 K for $x \sim 0.08$. These two samples showed well-defined ferromagnetic hysteresis curves at 5 K (see Fig. 5c). The M–H curve for $x \sim 0.04$ may roughly be approximated by assuming a spontaneous magnetization of ~0.2 μ_B/Ni plus a linear contribution. The spontaneous magnetization increases to ~0.3 μ_B/Ni for $x \sim 0.08$.

In Fig. 6a the H/M data measured at $H = 10^4$ Oe for these four samples are plotted. It is clear that the linear region shifts to the right with increasing x. These regions were fitted to the Curie–Weiss law as shown with the solid lines in Fig. 6a, and the parameters are plotted against x in Fig. 6b. The Weiss temperature increases quickly as x increases, while the effective Bohr magneton number remains almost constant.

4. DISCUSSION

The experimental results described above provide us with useful information concerning how the preparative conditions of this practically important but delicate system are reflected in magnetic properties. We will discuss this point below first.

We assume that a Ni ion substituted at the 3*a* site brings about a local but strong inter-NL communications as stated already and that the temperature of any resulting magnetic anomaly will be raised as Ni(3*a*) content, x, increases because of the tendency toward three dimensionality in magnetism. However, we should keep it in mind that the Ni(3*a*)(Ni(3*b*))$_6$ cluster would probably include two divalent ions for the sake of charge compensation, one at the 3*a* site and the other at the 3*b* site, and that this might

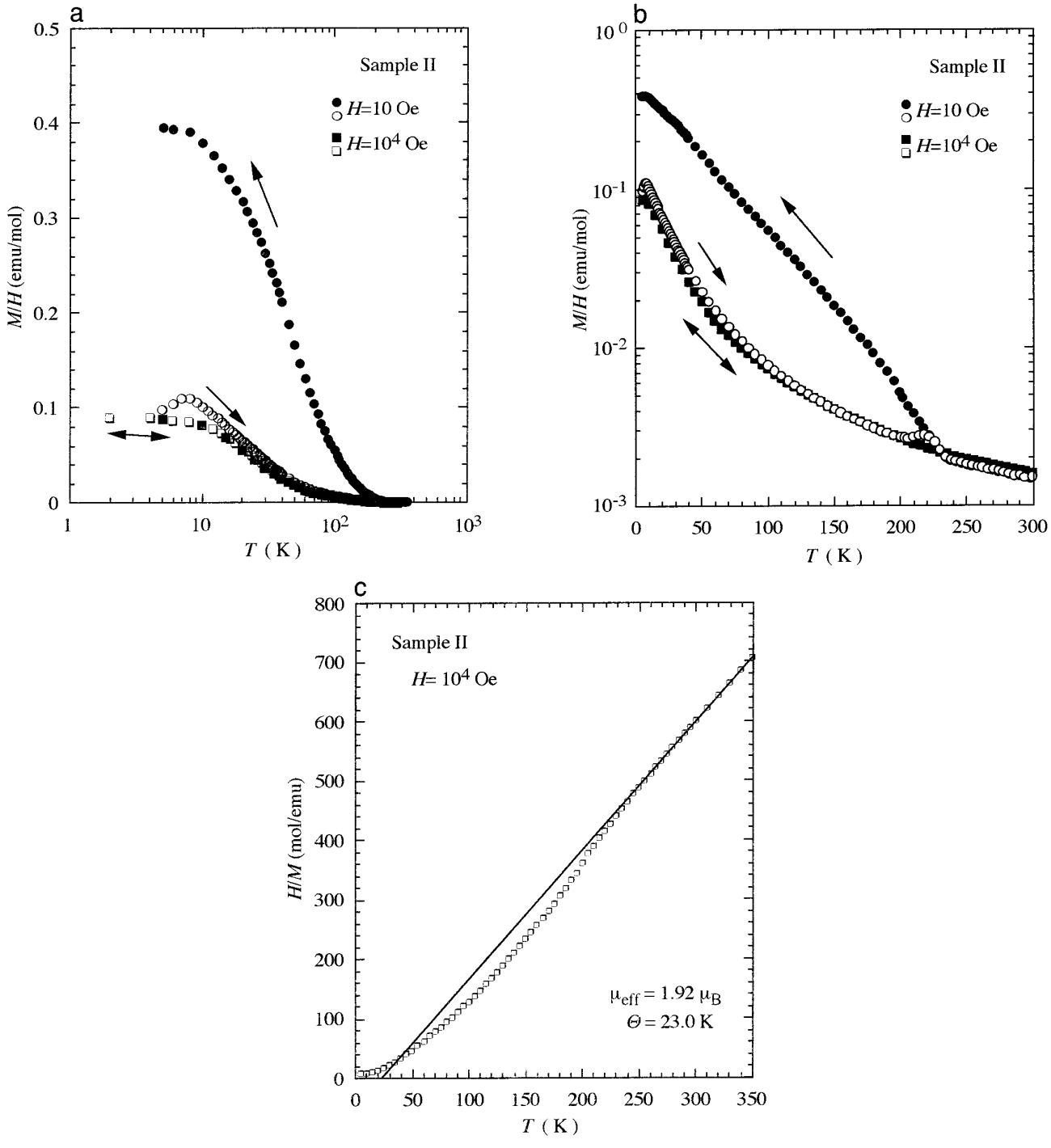

FIG. 4. (a) Temperature dependence of magnetization for sample II ($x \lesssim 0.01$) prepared at 650°C from Li_2O_2 and $Ni_{1.0}O$. The marks used are the same as in Fig. 3a. (b) Restyling of Fig. 4a with linear T scale and logarithmic M/H scale. The hysteretic magnetic anomaly appearing around 220 K can be clearly seen. (c) H/M at $H = 10^4$ Oe for sample II. The linear line represents Curie–Weiss behavior with $\mu_{eff} = 1.92\ \mu_B$ and $\Theta = 23.0$ K.

make the intracluster interaction complicated. It is interesting to note here that the spontaneous magnetization of $\sim$0.2 μ_B/Ni for $x \sim 0.04$ and 0.3 μ_B/Ni for $x \sim 0.08$ estimated from the M–H data at 5 K (Fig. 5c) are not far from the values estimated for ferrimagnetic clusters like $[3Ni^{3+}(3b, 1\ \mu_B, \uparrow)]$–$Ni^{2+}(3a, 2\ \mu_B, \uparrow\uparrow)$–$\{Ni^{2+}(3b, 2\ \mu_B, \downarrow\downarrow) + 2Ni^{3+}(3b, 1\ \mu_B, \uparrow)\}$, where [] and {} express the upper NL and the lower NL, respectively, or vice versa.

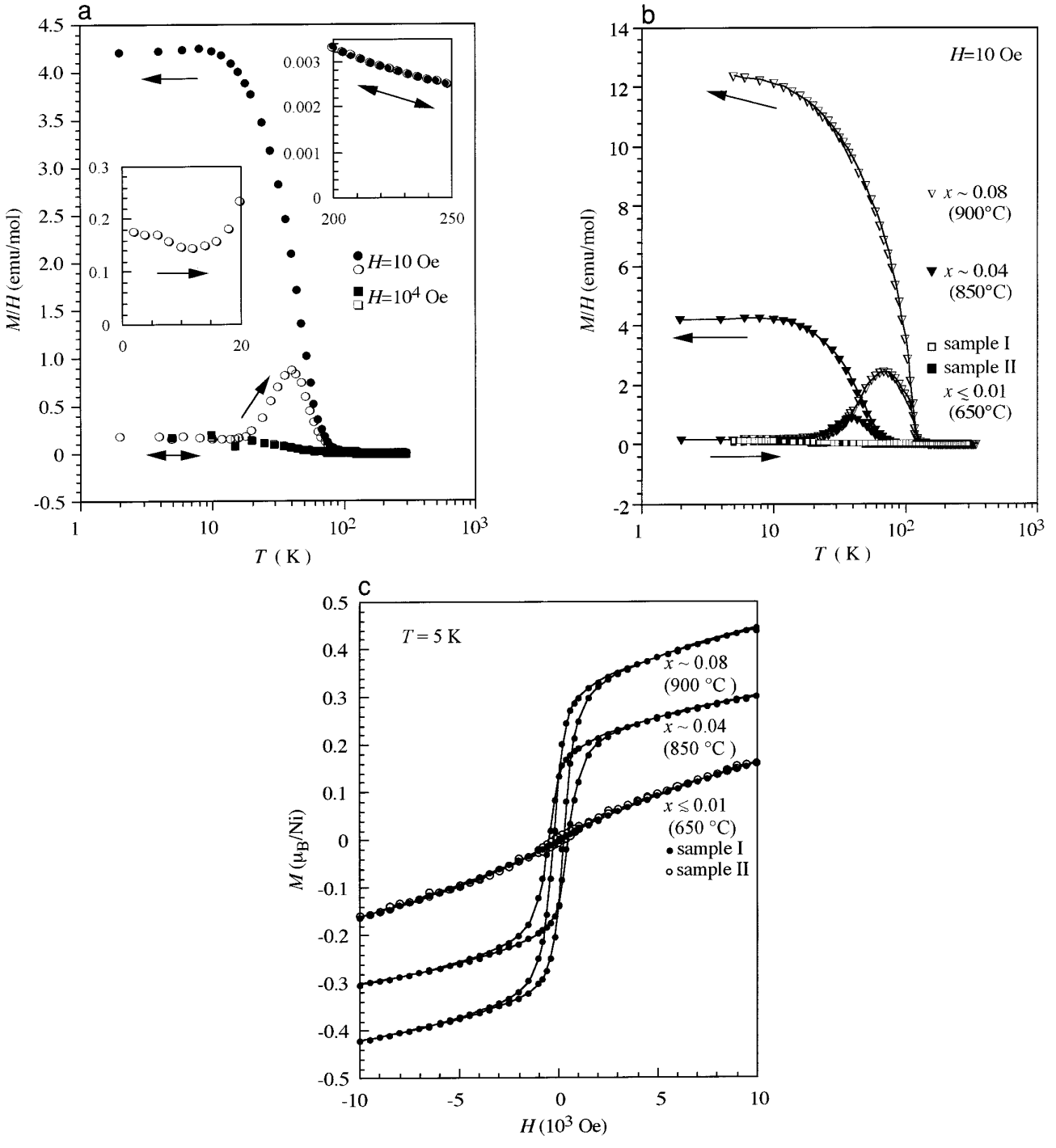

FIG. 5. (a) Temperature dependence of magnetization for a sample with $x \sim 0.04$ prepared at 850°C from Li_2O_2 and $Ni_{1.0}O$. Insets are partial extensions of this figure. The marks used are the same as in Fig. 3a. (b) Sample dependence of magnetization measured at $H = 10$ Oe after zero-field cooling and on field cooling for $x \sim 0.04$ and 0.08. The solid curvatures are guides for the eyes. (c) Field dependence of magnetization at 5 K. The samples were zero-field cooled down to 5 K and field was applied stepwise up to $\pm 10^4$ Oe. The initial lines are omitted.

The $Ni^{2+}(3a)$–O^{2-}–$Ni^{2+}(3b)$ interaction is assumed to be antiferromagnetic as in NiO, while the ferromagnetic $Ni^{2+}(3a)$–O^{2-}–$Ni^{3+}(3b)$ interaction may be explained by rewriting the bond as $Ni^{2+}(3a, \uparrow\uparrow)$–$O^{-}(2p_x^2 2p_y^2 2p_z, \downarrow)$–$Ni^{2+}(3b, \uparrow\uparrow)$ (z // the bond direction) in which the role of an oxygen hole leading to the ferromagnetic interaction is shown explicitly. The cluster moment of 5 μ_B thus estimated corresponds to an averaged moment of 0.2 μ_B/Ni

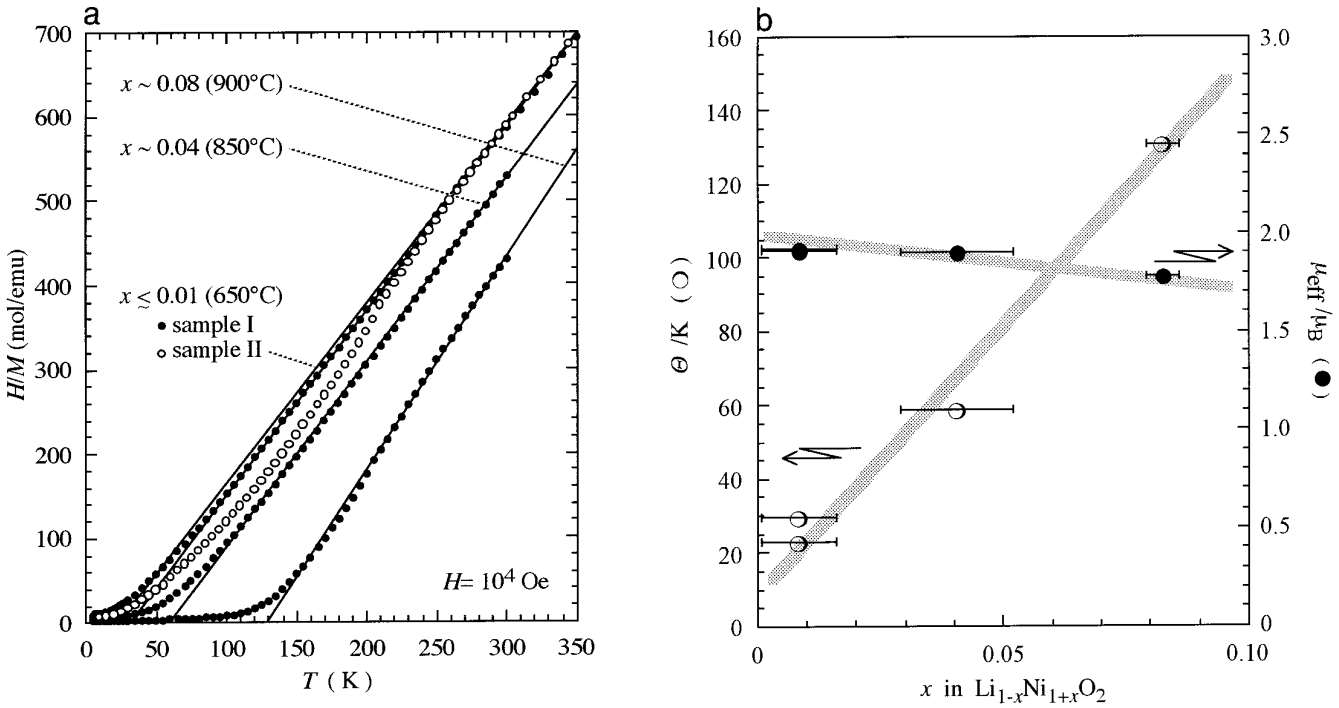

FIG. 6. Sample dependence of H/M at $H = 10^4$ Oe. The solid lines represent Curie–Weiss behavior with parameters given in Fig. 6b. (b) Sample dependence of Θ and μ_{eff} calculated from the data shown in Fig. 6a. The error bars represent the uncertainty in composition shown in Fig. 2. The thick dotted lines are guides for the eyes.

for $x \sim 0.04$ and 0.4 μ_B/Ni for $x \sim 0.08$. The present suggestion premises that the residual Ni(3*b*) ions, which are not involved in the clusters, contribute to the linear part of the M–H curves at 5 K.

The importance of the ferromagnetic inter-NL coupling mediated by Ni(3*a*) ions can be seen in the rapid increase of the Weiss temperature with increasing x (Fig. 6a), while the increase of the temperature of the ferromagnetic anomaly from 100 K for $x \sim 0.04$ to 140 K for $x \sim 0.08$ (Fig. 5b) indicates that intercluster interactions increase with x. The relatively high Weiss temperatures reported by Hirota *et al.* and Kemp *et al.* seem to have resulted from the presence of 4–5% Ni ions in the LLs.

Sample II does not follow the above line in a sense that it shows an anomaly at a higher temperature of ~240 K in spite of its lower Ni(3*a*) content. This contradiction can be explained by assuming the presence of a small amount of impurity phase of low Li content resulting from insufficient reactivity of coarse $Ni_{1.0}O$ grains at 650°C. Ganguly *et al.* reported an abrupt increase in magnetization between 260 and 230 K for $Li_{0.3}Ni_{0.7}O$ ($x = 0.4$) (20). The assignment of the 240-K anomaly to such an impurity phase, not to $LiNiO_2$ itself, is consistent with preliminary results of μSR (21) and ^{7}Li-NMR (22) measurements which do not detect any corresponding anomaly around 240 K. To be noted here is a possibility that such an impurity might form also in the process of thermal loss of Li from $LiNiO_2$ at high temperatures. This may be one of the reasons why the 240-K anomaly has been reported generally.

To be discussed next is how the present study contributes to the clarification of the genuine magnetism of $LiNiO_2$. We believe that sample I is the best sample ever obtained because it has the simplest magnetic behavior ever observed. It follows the Curie–Weiss law down to 80 K, and the effective Bohr magneton number is consistent with the isotropic $S = 1/2$ picture of $Ni^{3+}(t^6e^1)$ or its equivalent $Ni^{2+}(t^6e^2)\underline{L}$. We assume straightforwardly that the positive Weiss temperature indicates the ferromagnetic nature of the intra-NL nearest-neighbor interaction. Consideration of the Hunt coupling of a pair of holes on two mutually orthogonal $2p$ orbits on the same oxygen site would support this interpretation theoretically (23). Then, $LiNiO_2$ should show a long range ferromagnetic or antiferromagnetic ordering depending upon whether the dominant inter-NL interaction is ferromagnetic or antiferromagnetic. The simplest interpretation along this line of the T, H-dependence of magnetization shown in Figs. 3a, 3c, and 5c would be such that intra-NL ferromagnetic short range ordering develops below ~20 K leading to the nonlinear M–H relation and then inter-NL antiferromagnetic correlation results in an antiferromagnetic 3D ordering at ~8 K. However, to our surprise, there are no clear signs indicative of long range ordering in the measurements of specific heat, μSR (21), and ^{7}Li-NMR (22) on sample I.

As will be reported elsewhere in detail, the NMR study (22) reveals that sample I is still locally imperfect. The imperfections cause a local spin-glass like behavior, which is observed as the 8-K anomaly in the present magnetization measurement, while the clean parts (~80% in volume) remain paramagnetic down to at least 1.2 K. The μSR measurements also tell us that Ni spins remain fluctuating even at 20 mK. We believe that there is a new mechanism leading even ideal $LiNiO_2$ to a new type of magnetically disordered ground state as suggested below.

The Ni^{3+} ion, or the Ni^{2+} $\underline{L}$ complex, located at the 3*b* site of D_{3d} symmetry has a twofold degenerate orbital state of e_g symmetry. However, there is no sign of the degeneracy being lifted by a static cooperative Jahn–Teller distortion in our XRD and ND measurements made down to 10 K. As far as the orbital state remains degenerate, we should take the effects of orbital–spin coupling on magnetism into consideration explicitly. This is a coupling between orbital and spin structures, which should be distinguished from the usual on-site spin-orbit coupling (24).

Two neighboring Ni ions will gain energy when they assume two different orbital states (antiferro-orbital coupling) and the same spin state (ferromagnetic spin coupling), while the combination of ferro-orbital coupling and ferromagnetic spin coupling would be the highest energy state because electron transfer between the Ni ions is suppressed. Combinations of antiferromagnetic spin coupling with ferro- or antiferro-orbital coupling are intermediate (25, 26). However, it should be emphasized here that the antiferro-orbital coupling is frustrated within the present triangular NL and there can be no long-range orbital ordering (27, 28) as well-known for an antiferromagnetically frustrated triangular spin system. Orbital fluctuations thus caused will in turn disrupt the ferromagnetic spin ordering, because local and instantaneous ferro-orbital coupling reinforced by the frustration induces antiferromagnetic spin–spin coupling.

The applicability of the above mentioned theoretical idea should be examined quantitatively in the future. We believe that $LiNiO_2$ might be a new stage of quantum physics where the twofold degenerate orbital states and the twofold degenerate spin states are coupled with each other.

5. CONCLUSION

Measurements of magnetization as a function of field, temperature, and thermomagnetic history are shown to be quite useful for characterization of the quality of $LiNiO_2$. This is because the presence of excess Ni ions at the Li site causes ferromagnetic anomalies which can be detected easily by magnetometry. Ideal $LiNiO_2$ might provide us with a new stage of quantum physics of orbital–spin coupling. Efforts to prepare samples of even higher qualities are highly desirable, on which different measurements providing us with macroscopic, microscopic, static, and dynamic information concerning the electronic state and crystal structure should be made down to extremely low temperatures.

ACKNOWLEDGMENTS

We appreciate discussions with Professors Y. Kitaoka, A. Fujimori, Y. J. Uemura, F. C. Zhang, and Dr. K. Kojima. We express our gratitude to Professor Y. Kitaoka for providing us with his NMR results before publication and to Professor Uemura and Dr. Kojima for showing us μSR results before publication. The possibility of the frustration in orbital ordering in $LiNiO_2$ was first pointed out by Professor F. C. Zhang when he visited us in the summer of 1994. This study was partly supported by Grant-in-aids for Scientific Research on Priority Areas "Dynamics of fast ions in solids and its evolution for solid state ionics (no. 260)" and "Anomalous metallic state near the Mott transition (no. 258)" of the Ministry of Education, Science, and Culture, Japan and also a grant-in-aid of Nippon Sheet Glass Foundation for Materials Science (the 16th, 1994).

REFERENCES

1. J. R. Dahn, U. von Sacken, and C. A. Michal, *Solid State Ionics* **44,** 87 (1990).
2. R. Kanno, H. Kubo, Y. Kawamoto, T. Kamiyama, F. Izumi, Y. Takeda, and M. Takano, *J. Solid State Chem.* **110,** 216 (1994).
3. H. Arai, S. Okada, H. Ohtsuka, M. Ichimura, and J. Yamaki, *Solid State Ionics* **80,** 261 (1995).
4. J. B. Goodenough, D. G. Wickham, and W. J. Croft, *J. Phys. Chem. Solids* **5,** 107 (1958).
5. K. Hirakawa, H. Kadowaki, and K. Ubukoshi, *J. Phys. Soc. Jpn.* **54,** 3526 (1985).
6. J. P. Kemp, P. A. Cox, and J. W. Hodby, *J. Phys., Condens. Matter* **2,** 6699 (1990).
7. K. Hirota, Y. Nakazawa, and M. Ishikawa, *J. Phys., Condens. Matter* **3,** 4721 (1991).
8. J. N. Reimers, J. R. Dahn, J. E. Greedan, C. V. Stager, G. Liu, I. Davidson, and U. von Sacken, *J. Solid State Chem.* **102,** 542 (1993).
9. A. Hirano, R. Kanno, Y. Kawamoto, Y. Takeda, K. Yamaura, M. Takano, K. Ohyama, M. Ohashi, and Y. Yamaguchi, *Solid State Ionics* **78,** 123 (1995).
10. P. Kuiper, G. Kruizinga, J. Ghijisn, G. A. Sawatzky, and H. Verweij, *Phys. Rev. Lett.* **62,** 221 (1989).
11. M. A. van Veenendaal, and G. A. Sawatzky, *Phys. Rev. B* **50,** 11326 (1994).
12. T. Mizokawa, H. Namatame, A. Fujimori, K. Akeyama, H. Kondoh, H. Kuroda, and N. Kosugi, *Phys. Rev. Lett.* **67,** 1638 (1991).
13. J. B. Goodenough, "Magnetism and the Chemical Bond." Wiley–Interscience, New York, 1963.
14. P. S. Aggarwal and A. Goswami, *J. Phys. Chem.* **65,** 2105 (1961).
15. D. P. Bogatsky, *Zhur. Obshchei Khim.* **21,** 9 (1951).
16. F. Izumi, "The Rietveld Method" (R. A. Young, Ed.), Chap. 13. Oxford Univ. Press, Oxford, 1993.
17. C. Domb and M. F. Sykes, *Proc. R. Soc.* (*London*) *A* **240,** 214 (1957).
18. G. Rushbrooke and P. J. Wood, *Mol. Phys.* **1,** 257 (1958).
19. C. Domb and M. F. Sykes, *Phys. Rev.* **128,** 168 (1962).
20. P. Ganguly, V. Ramaswamy, I. S. Mulla, R. F. Shinde, P. P. Bakare, S. Ganapathy, P. R. Rajamohanan, and N. V. K. Prakash, *Phys. Rev. B* **46,** 11595 (1992).
21. K. Kojima and Y. J. Uemura, in preparation.
22. H. Wakabayashi, G.-q. Zheng, K. Ishida, Y. Kitaoka, and K. Asayama, in preparation.

23. G. A. Sawatzky, private communication.
24. T. M. Rice, "Spectroscopy of Mott Insulators and Correlated Metals" (A. Fujimori, and Y. Tokura, Eds.), p. 221. Springer-Verlag, Berlin, 1995; and references therein.
25. L. M. Roth, *Phys. Rev.* **149,** 306 (1966).
26. L. M. Roth, *J. Appl. Phys.* **38,** 1365 (1967).
27. F. C. Zhang, private communication.
28. A. Fujimori, private communication.